Electrical conductivity and thin-film growth dynamics

G. Palasantzas
Department of Applied Physics, Materials Science Center, University of Groningen, Nijenborgh 4, 9747 AG Groningen, The Netherlands

Y.-P. Zhao, G.-C. Wang, and T.-M. Lu
Department of Physics, Applied Physics, and Astronomy, and Center for Integrated Electronics and Electronics Manufacturing, Rensselaer Polytechnic Institute, Troy, New York 12180-3590

J. Barnas
Institute of Physics, Adam Mickiewicz University, ul. Umutowska 85, 61-614 Poznan, Poland

J. Th. M. De Hosson
Department of Applied Physics, Materials Science Center, University of Groningen, Nijenborgh 4, 9747 AG Groningen, The Netherlands
(Received 7 April 1999; revised manuscript received 2 December 1999)

It is known that surface steps can give rise to diffusion barriers and generate moundlike rough surfaces during thin-film growth. We study the influence of moundlike rough surfaces on electron scattering and electrical conductivity of semiconducting and metallic thin films. For a semiconducting film, the intraminiband cutoff q_c limits the contribution from mound surface scattering. Three different cases are illustrated to show how surface morphology affects the conductivity: $q_0<q_c$, $q_0=q_c$, and $q_0>q_c$. Here q_0 is the ring position of the surface power spectrum. For a metallic film with a single rough boundary, quantum size effect (QSE) oscillations are shifted in phase and weakened by the presence of wavelength selection in surface morphology. In this case, the conductivity reaches a minimum at a certain value of the system correlation length ζ when the mound separation λ obeys the condition $\lambda>\lambda_F$ or $\lambda<\lambda_F$ (λ_F being the Fermi wavelength). The presence of cross correlation in films with two rough boundaries greatly influences the initial stage of QSE oscillation of metallic films. Finally, we show that the size and shape of quantum effects depend very much on the different growth modes. The power-law behavior of the conductivity versus film thickness can be dramatically altered during dynamic growth, which provides a reasonable explanation for recent experiments.

I. INTRODUCTION

When the thickness of a smooth and continuous conducting film is reduced in one direction, the component of the wave vector q of electrons in this direction becomes quantized. This leads to the quantum size effect (QSE) which can affect the electrical conductivity.[1] Also the surface of a thin film adds additional electron scattering and has a significant influence on the film conductivity (the so-called classical size effect[2] (CSE)). The presence of rough boundaries in thin films can strongly influence QSE in the electrical transport properties. Jalochowski *et al.* found that the resistivity of ultrathin Pb films and Pb-In alloyed films on Si(111)(6×6)-Au (Ref. 3) and ultrathin Au films on Si(111)(7×7) (Ref. 4) has a 1 ML-periodic oscillations versus thickness due to the periodic change of the surface roughness. In the Pb and Pb-In systems additional 2 ML-period oscillations due to the QSE (Ref. 1) were observed. Oscillations in resistivity vs thickness were also observed in Pt films,[5] superposed metal films of Ag, In, and Ga on 20 nm-thick base of Ag or Au.[6] Luo *et al.* observed that the conductivity of epitaxial Ag films/24 nm Ag base/Si(111)(7×7) is proportional to the square of the interface width w and also has a complicated relationship with lateral correlation length ξ.[7] For quantum wells, Sakaki *et al.* showed experimentally and theoretically that the mobility of the two-dimensional electrons in modulated-doped AlAs/GaAs quantum wells is proportional to L^{-6}, where L is the width of the quantum well.[8] It was also shown that agreement between theoretical calculations and experimental data on the Hall mobility of metal-oxide semiconductor field effect transistor devices[9] and in the electron mobility of high-mobility Si(001) inversion layers[10] improves if the exponential correlation length at the Si-SiO_2 interface is taken into account. The interface roughness has also been shown to affect the electron subband of InAs/GaSb semiconducting quantum wells.[11]

On the theoretical side, there exist many studies of the influence of roughness on electrical resistivity using quantum-mechanical treatments.[12–18] Fishman and Calecki showed a power law behavior of thickness-dependent conductivity, $\sigma \propto d^s$.[14] If the lateral correlation length ξ and the electron Fermi wave vector q_F satisfies $\xi q_F \ll 1$, then $s=2.1-2.3$ for a metal film, which describes the $CoSi_2$ thickness-dependent conductivity data well.[19] For a semiconducting film $s=6$, which is consistent with the thickness dependent electron mobility data of AlAs/GaAs quantum well taken by Sakaki *et al.*[8] However, the roughness correlation function has a significant effect on the conductivity when $\xi q_F>1$. They have shown that when ξq_F increases from less than one to larger than one, s decreases from 2.3 to 1.5.[14] Recently these works were extended to self-affine surfaces,[18] where a roughness exponent H $(0<H<1)$ describes the fractality of a self-affine surface/interface. It has been shown theoretically that the value of H significantly influences elec-

tron transport properties of metallic and semiconducting thin films.[18] More specifically, the roughness exponent H influences not only the size and shape of QSE oscillations, but also the magnitude of the film conductivity.

So far most theories of roughness effect on electrical resistivity only assume that the surface roughness is fixed when the film thickness changes. This condition is not satisfied in most experimental situations. The roughness usually varies during the growth process, for example, as shown in both the layer-by-layer growth of Pb and Au films[3,4] and the epitaxial Ag films.[7] The change in the surface roughness of a film and the increase of the film thickness are governed by the same dynamic growth process, and are very closely related to each other. For a perfectly smooth surface, the increase of film thickness tends to increase the conductivity of the film. However, the increase of the roughness tends to reduce the conductivity due to the boundary scattering. Therefore, the behavior of the conductivity as a function of thin film growth time t or thickness d is a result of the competition between the thickness increment and the roughness variation (assuming that effects due to scattering by impurities, defects, and grain boundaries can be neglected). Under different film preparation conditions (substrate temperature, pressure, and growth rate), or different growth methods (physical vapor evaporation, sputtering, chemical vapor deposition, etc.), one may obtain a wide variety of different surface morphologies as well as the dynamic behaviors which are inherently related to different growth mechanisms. For example, in the epitaxial growth of a film, the layer-by-layer growth mode can commence in some cases, within a certain temperature regime, where each depositing layer is completed before the growth of the next layer starts.[20] However, such a growth mode may not always occur. Instead growth fronts with rough multilayer step structures in the form of mounds (unstable growth) could form during growth.[21–24] This is the result of the existence of an asymmetric step-edge diffusion barrier or Schwoebel barrier, which inhibits the downhill diffusion of incoming atoms in this multilayer step structure. In contrast, the noise-induced roughening during the growth can lead to the formation of self-affine fractal morphology.[23]

One can imagine that a different dynamic growth process can give a different thickness-dependent or a growth-time dependent behavior of the conductivity. A simple example is to assume that the thickness scales as $d \propto t$, the interface width as $w \propto t^{\beta}$, and the conductivity as $\sigma \propto d^{s} w^{-2}$.[14] Substituting the first two relations into the third one, one finds $\sigma \propto t^{s'} = t^{s-2\beta}$. This means that the general power-law relation $\sigma \propto d^{s}$ with $s = 2.3$ or 6.0 may not be observed because the combination of power-law growth $w \propto t^{\beta}$ and the time-dependent thickness $d \propto t$ reduces the exponent value of the conductivity from s to $s' = s - 2\beta$. Up to now, most of those dynamic growth effects have not been considered in the thickness-dependent conductivity. Also previous theoretical works did not consider how different kinds of morphology would affect the surface conductivity. Moreover, the effects of roughness in films with two rough boundaries as well as the cross correlation arising from roughness correlation between film/substrate and film/vacuum interfaces on the electrical conductivity have not been considered yet.

In this paper, we correlate phenomenological roughness correlation models with the thin film conductivity. We show that the dynamic growth process does alter the conductivity vs thickness behavior. The paper is organized as follows. First, we formulate the equations describing the double boundary effect on the conductivity in Secs. II and III. Then, we investigate the effect of a single rough mound boundary on the conductivity of semiconducting and metalic films in Sec. IV. For semiconducting films the quantum transport formula can be simplified, and provides a basic starting point to understand the morphological effect. In this section we also discuss the conductivity of metallic films with a single mound surface. In Sec. V, we concentrate on the dynamic growth effect (unstable and stable) on the conductivity of metallic films grown on a rough mound substrate (double rough boundaries). A conclusion is made in Sec. VI.

II. CONDUCTIVITY THEORY FOR THIN FILMS WITH TWO ROUGH BOUNDARIES

When the bulk electron mean free path is much longer than the film thickness, the electrical conductivity is properly described by those formalisms which take into account quantum-mechanically electronic structure of the film.[14] For simplicity, we assume a model electronic structure based on free electron approximation and ignore bulk scattering processes. Thus, electrons are scattered diffusively only on rough interfaces. In the following, we consider a film of average thickness d with two rough interfaces distinguished by the index $b=(1,2)$ located at $z_b(\mathbf{r}) = z_b + h_b(\mathbf{r})$ ($z_1 = -d/2$ and $z_2 = d/2$). Here, the $h_b(\mathbf{r})$ are the random roughness fluctuations which are assumed to be single-valued functions of the in-plane position vector $\mathbf{r}=(x,y)$. For each interface we assume an isotropic auto-correlation function $C_b(\mathbf{r}) = \langle h_b(\mathbf{r}) h_b(0) \rangle$ with $\langle h_b(\mathbf{r}) \rangle = 0$, and a cross correlation function $C_{bb'}(\mathbf{r}) = \langle h_b(\mathbf{r}) h_{b'}(0) \rangle$ with $b \neq b'$. In the Born approximation the in-plane conductivity is given by[14]

$$\sigma = \frac{4e^2}{\hbar d} \sum_{v=1}^{N} \sum_{v'=1}^{N} (E_F - \varepsilon_v)(E_F - \varepsilon_{v'}) [C(E_F)_{vv'}]^{-1}, \tag{1}$$

with the matrix elements $[C(E_F)]_{vv'} (= [C^{\mathrm{in}}(E_F)]_{vv'} + [C^{\mathrm{cor}}(E_F)]_{vv'})$ describing intra- and intersubband transitions. The matrix elements are equal to the sum of an incoherent term C^{in} (incoherent scattering by two rough interfaces) and cross correlation term C^{cor} terms (coherent scattering by different interfaces). In Eq. (1), N is the number of occupied minibands, and E_F is the Fermi energy.

The matrix elements $[C^{\mathrm{in}}(E_F)]_{vv'}$ of the coherent part of scattering were calculated in Refs. 25 and 26, and their extensions to the case of a single layer film with double rough boundaries (ignoring any spin-splitting effects) take the form

$$[C^{\mathrm{in}}(E_F)]_{vv'} = \sum_{b=1}^{2} \left[\delta_{vv'} \sum_{\mu=1}^{N} q_v^2 L_b^{v\mu} \int_0^{2\pi} \langle |h_b(q_{v\mu})|^2 \rangle d\theta - q_v q_{v'} L_b^{vv'} \int_0^{2\pi} \langle |h_b(q_{vv'})|^2 \rangle \cos\theta d\theta \right], \tag{2}$$

with $L_b^{v\mu}=U_b^2\psi_v^2(z_b)\psi_\mu^2(z_b)$. $\langle|h_b(q)|^2\rangle$ is the Fourier transform of the auto-correlation function $C_b(r)$ (assuming isotropic roughness), $q_{vv'}=(q_v^2+q_v^2-2q_vq_{v'}\cos\theta)^{1/2}$, $q_v=[(2m/\hbar^2)(E_F-E_v)]^{1/2}$ and is the wave vector of the v miniband edge, θ is the angle between $\mathbf{q}_v$ and $\mathbf{q}_{v'}$, $\psi_v(z)$ is the quantized electron wave function in the z direction for a film with smooth boundaries, and U_b is the confining potential at the bth interface.[14] The matrix elements of the cross-correlated part are calculated in a similar way but for indices $b\neq b'$.[27] Thus, we have

$$[C^{\rm cor}(E_F)]_{vv'}=2\left[\delta_{vv'}\sum_{\mu=1}^{N}q_v^2L_{12}^{v\mu}\int_0^{2\pi}\langle|h_{12}(q_{v\mu})|^2\rangle d\theta - q_vq_{v'}L_{12}^{vv'}\int_0^{2\pi}\langle|h_{12}(q_{vv'})|^2\rangle\cos\theta d\theta\right], \tag{3}$$

with $L_{12}^{v\mu}=-[U_1\psi_v(z_1)\psi_\mu(z_1)][U_2\psi_v(z_2)\psi_\mu(z_2)]$. $\langle|h_{12}(q)|^2\rangle$ is the the Fourier transform of cross correlation function $C_{12}(r)$. The number of occupied minibands N and the Fermi level E_F for a film of given thickness d and electron density n are determined from the relation[18] $nd=(m/\pi\hbar^2)(NE_F-\Sigma_{v=1}^{N}E_v)$ with the areal electron density $n_s=nd$. If the electrons are localized in the film by an infinite confining potential well ($U_b\rightarrow+\infty$), then the edge of the vth miniband is given by $E_v=(\hbar^2/2m)(v\pi/d)^2$ (Refs. 14 and 18) with $L_b^{v\mu}=(h^2/4md^3)^2v^2\mu^2$ and $L_{12}^{v\mu}=-(h^2/4md^3)^2v^2\mu^2$. Note that the validity of the above conductivity formalism requires the roughness amplitude to be much smaller than the film thickness d ($w\ll d$).[8,14]

III. FOURIER TRANSFORM OF MOUND SURFACES

In order to correctly account for the cross correlations for films with double rough boundaries, we will consider the growth within the framework of linear Langevin growth equations. These equations have been shown to describe the growth mechanism reasonably well in various cases.[24] The roughened growth front is described by the linear equation

$$\partial h_2(\mathbf{r},t)/\partial t=Lh_2(\mathbf{r},t)+\eta(\mathbf{r},t), \tag{4}$$

with $\eta(\mathbf{r},t)$ being a Gaussian white noise such that $\langle\eta(\mathbf{r},t)\eta(\mathbf{r}',t')\rangle=2D\delta(\mathbf{r}-\mathbf{r}')\delta(t-t')$, $\langle\eta(\mathbf{r},t)\rangle=0$, D being the noise amplitude, and L being the linear operator $L=\pm v\nabla^2-\kappa\nabla^4$. The coefficient κ is proportional to the surface diffusion coefficient of incoming atoms during film growth. The coefficient v with a $(-)$ sign describing unstable growth due to Schwoebel barrier or a $(+)$ sign describing stable growth due to condensation/evaporation.[24] Performing a Fourier transform of Eq. (4) (Ref. 24) one obtains the roughness spectrum $\langle|h_2(\mathbf{q},t)|^2\rangle$ of the film/vacuum interface and the cross correlation roughness spectrum $\langle|h_{12}(\mathbf{q},t)|^2\rangle$

$$\langle|h_2(\mathbf{q},t)|^2\rangle=e^{2L(\mathbf{q})t}\langle|h_1(\mathbf{q},t)|^2\rangle+(8\pi)D(e^{2L(\mathbf{q})t}-1)L(\mathbf{q})^{-1}, \tag{5}$$

$$\langle|h_{12}(\mathbf{q},t)|^2\rangle=e^{L(\mathbf{q})t}\langle|h_1(\mathbf{q},t)|^2\rangle, \tag{6}$$

with $L(\mathbf{q})=\mp vq^2-\kappa q^4$, and $h_i(\mathbf{q},t)$ being the spatial Fourier transform of $h_i(\mathbf{r},t)$. Both spectra are necessary relations for further calculations of the film conductivity.

A moundlike rough morphology can also be described by a phenomenological height-height correlation function[24] $C(r)=w^2e^{-(r/\zeta)^2}J_0(2\pi r/\lambda)$ where its Fourier transform has the form[24]

$$\langle|h(q)|^2\rangle=(2\pi)(w^2\zeta^2/2)e^{-(4\pi^2+q^2\lambda^2)(\zeta^2/4\lambda^2)}I_0(\pi q\zeta^2/\lambda), \tag{7}$$

where $J_0(x)$ and $I_0(x)$ are the zeroth-order Bessel and modified Bessel functions, respectively. There are three roughness parameters in the model: the interface width w, the system correlation length ζ, which determines how randomly the mounds are distributed on the surface, and the average mound separation λ.[24] Combining both lateral length scales ζ and λ we can define an effective lateral correlation length ξ by the relation $(1/\xi^2)=(1/\zeta^2)+(\pi^2/\lambda^2)$. Note that the correlation function $C(r)$ has an oscillatory behavior for $\zeta\geqslant\lambda$ (strong Schwoebel effect) leading to a characteristic satellite ring at $q_0=2\pi/\lambda$ of the power spectrum $\langle|h(q)|^2\rangle$.[24]

IV. CONDUCTIVITY OF SEMICONDUCTING AND METALLIC FILMS WITH A SINGLE MOUND SURFACE

Semiconducting films. As the electron density n of a semiconducting film is very low, usually the number of occupied minibands N is small, say $N=1$ or 2. If we take $N=1$, the electrical conductivity can be analytically expressed as

$$\sigma=G_0\left\{\frac{4n}{\pi^2}\left[\int_0^{2\pi}(\langle h_1(q)^2\rangle+\langle h_2(q)^2\rangle-2\langle h_{12}(q)^2\rangle)\times(1-\cos\theta)d\theta\right]^{-1}\right\}d^6, \tag{8}$$

where $q=[4\pi nd(1-\cos\theta)]^{1/2}$, is the amplitude of scattered momentum transfer and $G_0=e^2/2\pi\hbar$. Equation (8) shows that only certain spatial frequency regime of the surface morphology will contribute to the conductivity. This follows from the fact that q ranges from 0 to an upper cutoff $q_c=\sqrt{8\pi nd}$, which is fixed for constant areal density nd. Equation (8) also shows that the forward electron scattering ($\theta\approx0$ or $\theta\approx2\pi$) does not contribute to the resistivity, while backward electron scattering ($\theta=\pi$) gives the dominant contribution.

Clearly from Eq. (8) we obtain the power-law behavior of the film conductivity versus film thickness as $\sigma\propto d^6$. Since the Fermi wavelength λ_F for a semiconducting film is usually large ($\sim$10 nm), the QSE oscillation for semiconducting films is not obvious as for metallic films. Therefore, in the following we only discuss the morphological issue on the conductivity of semiconducting films for mound roughness. For a single mound boundary we have $\langle h_1(q)^2\rangle=\langle h_{12}(q)^2\rangle=0$. Since $\langle|h_2(q)|^2\rangle=\langle|h(q)|^2\rangle\propto w^2$, the conductivity will depend on the roughness amplitude w simply as $\sigma\propto w^{-2}$, while any other complex dependence will arise solely from the dependence on the roughness parameters λ and ζ. Note also that the validity of the above conductivity formalism requires the roughness amplitude to be much smaller than the film thickness d ($w\ll d$).[8,14]

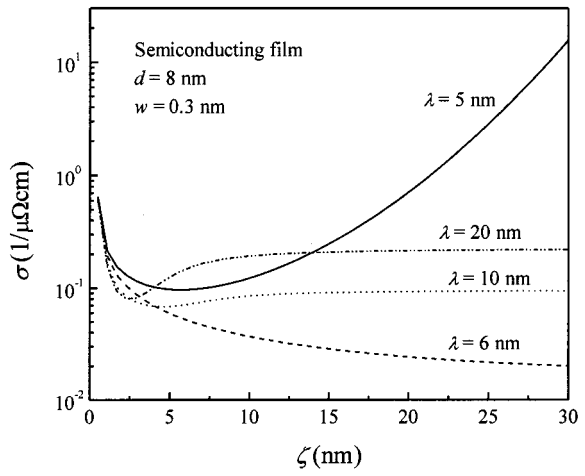

FIG. 1. Semi-log plot of the conductivity σ of a semiconducting film vs system correlation length ζ for film thickness $d=8$ nm area electron density $n_s=4.8\times10^{-2}\,\mathrm{nm}^{-2}$, interface width $w=0.3$ nm, and average mound separations $\lambda=5$, 6, 10, and 20 nm.

If we assume that the surface of a semiconducting film has a mound morphology with the power spectrum given by Eq. (7), $[h_2(q)=h(q)]$, we can calculate the conductivity according to Eq. (8). Figure 1 shows the conductivity of a semiconducting film as a function of the system correlation length ζ, for various values of average mound separation $\lambda=5$, 6, 10, and 20 nm. In this case the cutoff $q_c=1.1\,\mathrm{nm}^{-1}$, and the Fermi wave vector q_F is 0.7 nm^{-1}. For these four different values of the average mound separations, we observe different behaviors from Fig. 1: For $\lambda=5$ nm, the conductivity decreases at small system correlation length ζ, after it reaches a minimum, it increases dramatically. For $\lambda=6$ nm, the conductivity decreases monotonically with increasing ζ. However, for $\lambda=10$ and 20 nm, the ζ-dependent conductivity behavior is more complicated. In the small-ζ regime, the conductivity decreases with increasing ζ and after reaching a minimum it increases again and eventually saturates at a certain constant value for large ζ. The small-ζ dependence in all these four cases is the same. The behavior of the conductivity in all those four cases can be understood if we investigate the corresponding power spectra. Figure 2 shows the power spectra for $\lambda=5$, 6, and 10 nm in two different cases: (a) $\lambda=4\zeta$ and (b) $\lambda=\zeta$. In the case $\lambda=4\zeta$, there are only weak mounds on the surface, and the surface morphology is dominated by randomness, the power spectra look very similar to those of self-affine surfaces. As ζ increases, the power spectra become narrower, and their maximum amplitudes peak in the lower spatial frequency regime. The integral value in Eq. (8) (with $\langle h_1(q)^2\rangle=\langle h_{12}(q)^2\rangle=0$) increases, while the conductivity decreases. This is in agreement with observations from self-affine roughness.[14] In this case, the electron forward scattering dominates.

However, when ζ keeps on increasing, the ring appears and becomes sharper. According to the discussion in Sec. III, the corresponding ring positions are 1.25, 1.05, and 0.63 nm^{-1}, for $\lambda=5$, 6, and 10 nm, as shown in Fig. 2(b). Clearly those cases correspond to $q_0>q_c$, $q_0\approx q_c$, and $q_0<q_c$. In the case $q_0>q_c$, when the ring becomes sharp enough, the integral in Eq. (8) only covers part of the ring, and the value of the integration begins to decrease which leads to the conductivity increase. This turning point occurs at about $\zeta_{\min}=\lambda$. At very large ζ value, the ring becomes so sharp that it will be totally outside the integration limits, 0 to q_c, and the contribution of the surface roughness will be zero because the surface features are too small to scatter electrons. In the case $q_0<q_c$, when ζ increases at certain points, the integral region covers the entire power spectrum, the integral in Eq. (8) [with $\langle h_1(q)^2\rangle=\langle h_{12}(q)^2\rangle=0$] reaches the maximum value while the conductivity becomes minimum. This covers all the scattering events at all angles. At this point, we would expect $\zeta_{\min}\propto(q_c-q_0)^{-\tau}$, where our numerical calculation shows $\tau=1.46\pm0.08$. Therefore, when λ increases, $\zeta_{\min}$ should decrease, which is the case shown in Fig. 1 (see $\lambda=20$ nm). When ζ keeps on increasing, the power spectrum concentrates more around q_0, and the effective integration region in Eq. (8) decreases. This causes the increase of the conductivity. However, when ζ becomes very large, the power spectrum tends to become a δ function, and the conductivity becomes constant. In this case, the electron tends to

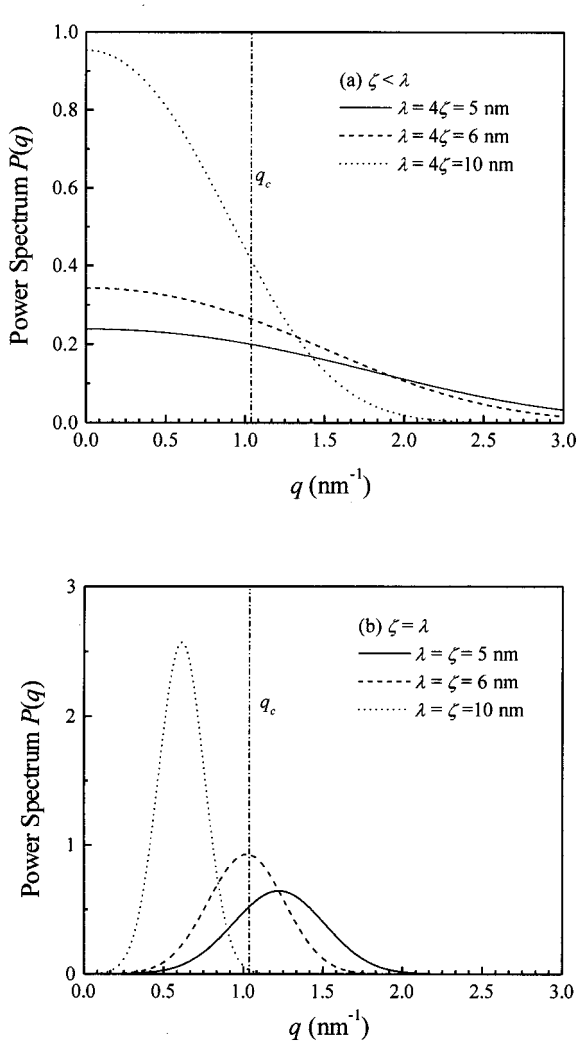

FIG. 2. The power spectra $P(q)$ of surfaces with $\lambda=5$, 6, and 10 nm for (a) $\lambda=4\zeta$, and (b) $\lambda=\zeta$. The straight lines in the figures represent the cutoff wave vector q_c of the electron intraminiband scattering.

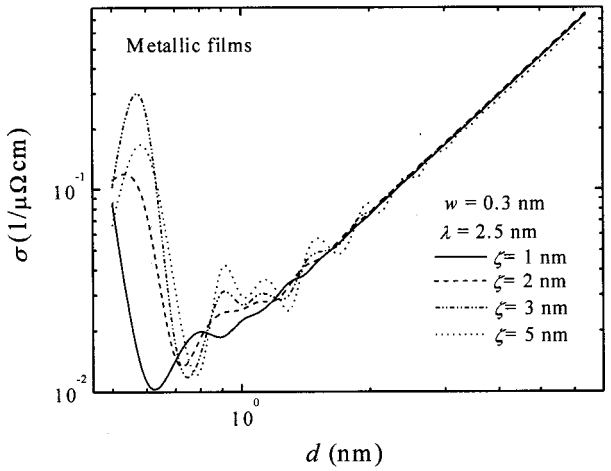

FIG. 3. Log-log plot of the conductivity σ of a metallic film vs film thickness d for $\lambda = 2.5$ nm, and various $\zeta = 1$, 2, 3, and 5 nm. Here $w = 0.3$ nm, electron density $n = 4.8 \times 10^1$ nm^{-3}.

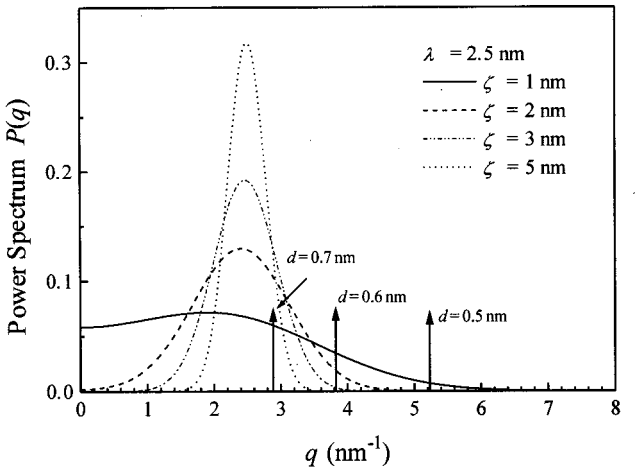

FIG. 4. The power spectra $P(q)$ of surfaces with $\zeta = 1$, 2, 3, and 5 nm for $\lambda = 2.5$ nm. The arrows in the figure stand for the positions of the minimum wave vector during interminiband scattering Δq_{12} for metal films with thickness $d = 0.5$, 0.6, and 0.7 nm.

be scattered into a certain angle, which is determined by q_0. As λ increases, q_0 decreases, and this constant value of the conductivity increases. This means more specular reflection of the electron occurs. In the case $q_0 = q_c$, when the ring appears, the integration always covers the lower half of the ring. As ζ increases, the power spectrum amplitude around q_0 (or q_c) increases. Consequently, the probability of backward scattering increases and the conductivity decreases. At very large ζ, the electron backward scattering dominates, and the conductivity becomes even smaller.

Metallic Films. Since the electron density for metallic films is very high, the number of occupied minibands N can be very large, $N \gg 1$. In this case we should use Eq. (1) to estimate the conductivity. First, let us consider a thin film with a single mound surface. Figure 3 shows the conductivity vs the film thickness d for metallic films with a carrier density $n = 4.8 \times 10^1$ nm^{-3}, a fixed interface width $w = 0.3$ nm, a fixed mound separation $\lambda = 2.5$ nm, and various system correlation lengths ζ. The corresponding Fermi wavelength is $\lambda_F \approx 0.52 - 0.57$ nm. There are pronounced QSE oscillations at small film thickness for various ζ values. Generally, a new cycle of the oscillations begins when the Fermi level crosses a miniband edge. This is associated with the opening of new channels for scattering, which leads effectively to a drop in the conductivity. The oscillation period is about half the Fermi wavelength ($\lambda_F/2 \approx 0.25$ nm). However from Fig. 3 we see that for $\zeta \ll \lambda$ ($\zeta = 1$ nm in Fig. 3), a weak mound surface, the calculated QSE oscillations with increasing film thickness are weak. As ζ increases, the phase of quantum size effect gradually changes (see the curve for $\zeta = 2$ nm in Fig. 3). When $\zeta > \lambda$, the phase shifts almost by π, and the oscillation amplitude reaches a maximum at $\lambda \approx \zeta$ (see the curve for $\zeta = 3$ nm in Fig. 3). After ζ becomes larger than λ, the phase of the oscillation changes a little with ζ, but the amplitude of the oscillation increases (see the curve for $\zeta = 5$ nm in Fig. 3). In this case, the mound morphology dominates the surface.

In order to understand this behavior, let us examine the thickness region for $d = 0.4$ nm to $d = 0.8$ nm. From Eq. (1), the conductivity come from both the intraminiband and interminiband scattering processes. The transition matrix only covers a certain spatial frequency region of the surface power spectrum, same as the discussion above. For the intraminiband scattering, the frequency region is from 0 to $2q_v$, while for the inter-miniband scattering it is from $\Delta q_{uv} = q_u - q_v$ to $q_u + q_v$. Table I shows the number of minibands N, the Fermi wave vector q_F, the miniband edge wave vector q_v, and the minimum wave vector during interminiband scattering Δq_{uv} for those thicknesses. Figure 4 shows the power spectra of a surface at $\lambda = 2.5$ nm and for various ζ values. In this case, the ring of the power spectrum q_0 positions at 2.51 nm^{-1}, which is far less than q_v shown in Table I. For $d = 0.4$ nm, $N = 1$, and $q_1 = 12.36$ nm^{-1}, which is well above q_0, the integral in Eq. (8) [with $\langle h_1(q)^2 \rangle = \langle h_{12}(q)^2 \rangle = 0$] covers the whole power spectrum, and the

TABLE I. The number of miniband N, the Fermi wave vector q_F, the miniband-edge wave vector q_v, and the minimum wave vector during interminiband scattering Δq_{uv} for different film thickness.

d (nm)	N	q_F (nm^{-1})	q_1 (nm^{-1})	q_2 (nm^{-1})	q_3 (nm^{-1})	Δq_{12} (nm^{-1})	Δq_{13} (nm^{-1})	Δq_{23} (nm^{-1})
0.4	1	14.65	12.36					
0.5	2	15.31	13.96	8.75		5.21		
0.6	2	13.72	12.68	8.87		3.81		
0.7	2	12.82	12.01	9.15		2.86		
0.8	3	13.27	12.67	10.69	6.09	1.98	6.58	4.6

conductivity for different ζ should be close. As discussed in the above, the conductivity vs the system correlation length ζ should behave similarly to the curve of $\lambda = 10$ nm in Fig. 1. From $d = 0.4$ nm to $d = 0.5$ nm, the Fermi energy crosses the second miniband, the conductivity should be a minimum. This is the case for most surfaces with $\zeta > \lambda$. However, for $\zeta < \lambda$, the conductivity is either at a maximum ($\zeta = 1$ nm curve at $d = 0.5$ nm in Fig. 3) or somewhere in the middle ($\zeta = 2$ nm curve at $d = 0.5$ nm in Fig. 3). This means the roughness of the surface does not contribute a lot to the conductivity. From $d = 0.5$ to 0.6 nm, since $q_v \gg q_0$, the contribution from the intraminiband scattering to the matrix element C_{vv} is almost the same. However, the interminiband scattering contribution is different. As shown in Table I the minimum wave vector during interminiband scattering Δq_{uv} decreases from 5.21 to 3.81 nm^{-1}. For a surface morphology with $\zeta \ll \lambda$, the interminiband integrations will increase, as do all the matrix elements C_{vv}, defined by Eq. (1). This requires a decrease in the conductivity. On the other hand, the increase of film thickness tends to increase the conductivity. In the case $\zeta = 1$ nm the roughness effect overcomes the thickness effect, and the conductivity decreases. But at $\zeta = 2$ nm, the thickness effect is dominant. For $\zeta > \lambda$, although Δq_{uv} decreases, it is still well outside the ring (see Fig. 4). Therefore, the contribution of the roughness to the matrix element at $d = 0.6$ nm is the same as that at $d = 0.5$ nm, and the increasing thickness requires the conductivity increase. When the film thickness increases from 0.6 to 0.7 nm, for $\zeta > \lambda$, the Δq_{uv} decreases into the power spectrum ring, and the roughness starts to contribute to the conductivity. Then the conductivity drops. For $\zeta \ll \lambda$, the roughness effect begins to decrease since more forward scattering contributes to the matrix elements. From $d = 0.7$ to 0.8 nm, the Fermi energy crosses the third miniband, and we should observe another cycle of oscillation. Therefore, the shift of phase from $\zeta \ll \lambda$ to $\zeta > \lambda$ is a reflection of the morphological transition from a nonmound surface to a mound surface.

For larger thickness, the conductivity can be approximated as a power law of the thickness, $\sigma \sim d^{s'}$, where the value of exponent s' varies in the range $s' \approx 1.91 - 1.97$. This value is lower than 2.3. This is expected since the effective lateral correlation length ξ is about $0.6 - 0.8$ nm, and $\xi q_F \approx 7.5 - 10 > 1$. In fact this result is consistent with Ref. 14, which showed that for $\xi q_F > 1$, $s < 2.3$.

V. CONDUCTIVITY OF METALLIC FILMS WITH DOUBLE ROUGH BOUNDARIES

Now let us add the substrate roughness effect on the film conductivity. In this case, we assume the substrate is a mound surface, and the metallic film grown on it follows either unstable growth or stable growth as discussed in Sec. III. The rough mound substrate is described by Eq. (7), the film/vacuum surface is described by Eq. (5), and the cross correlation by Eq. (6). The growth coefficients κ and v are assumed such that the surface and interface widths are much smaller than the film thickness. This restriction implies $v < \kappa$, and constrains the contribution of large length scales ($r > 2\pi\sqrt{v/\kappa}$) that is dominated by v (Schwoebel barrier or evaporation/condensation) relative to short length scale behavior ($r < 2\pi\sqrt{v/\kappa}$) that is controlled by κ (surface diffusion). These considerations are important for unstable growth to avoid a breakdown of the validity of the linear approximation. Our calculations were performed for a film growth rate $R = 0.2$ nm/s (yielding a film thickness $d = Rt$) and a noise amplitude $D = 3$. Moreover, the units of the coefficients D, κ, and v in the growth equations are assumed such that $[D] = $ Å/s, $[\kappa] = $ Å^4/s, and $[v] = $ Å^2/s.

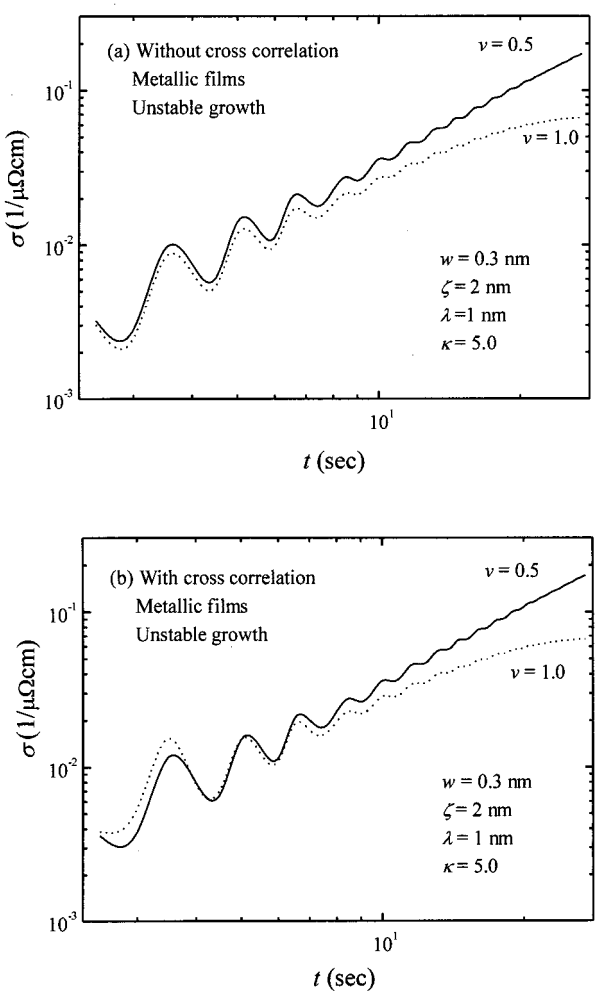

FIG. 5. Log-log plot of the conductivity σ of a thin metallic film vs growth time t (unstable growth) for different v values: $v = 0.5$, 1.0 (a) without cross correlation, and (b) with cross correlation contribution. Here, the roughness parameters of the substrate are $w = 0.3$ nm, $\zeta = 2$ nm, $\lambda = 1$ nm; and $\kappa = 5.0$, and the electron density $n = 4.8 \times 10^1$ nm^{-3}.

Unstable Growth. As shown in Fig. 5, in the unstable growth regime for substrate parameters $\zeta > \lambda$ the conductivity is very sensitive to the Schwoebel barrier coefficient v, affecting strongly the shape and size of time-dependent QSE oscillations, especially at longer growth time. For small v value ($= 0.5$), the conductivity increases almost as a power law with the growth time. However, for large v value ($= 1.0$), the conductivity increases much less than the case of small v value, also the absolute value of the conductivity drops. This effect indicates strong boundary roughness scattering with increasing coefficient v, and is in agreement with the fact that the surface becomes rougher with larger v value.

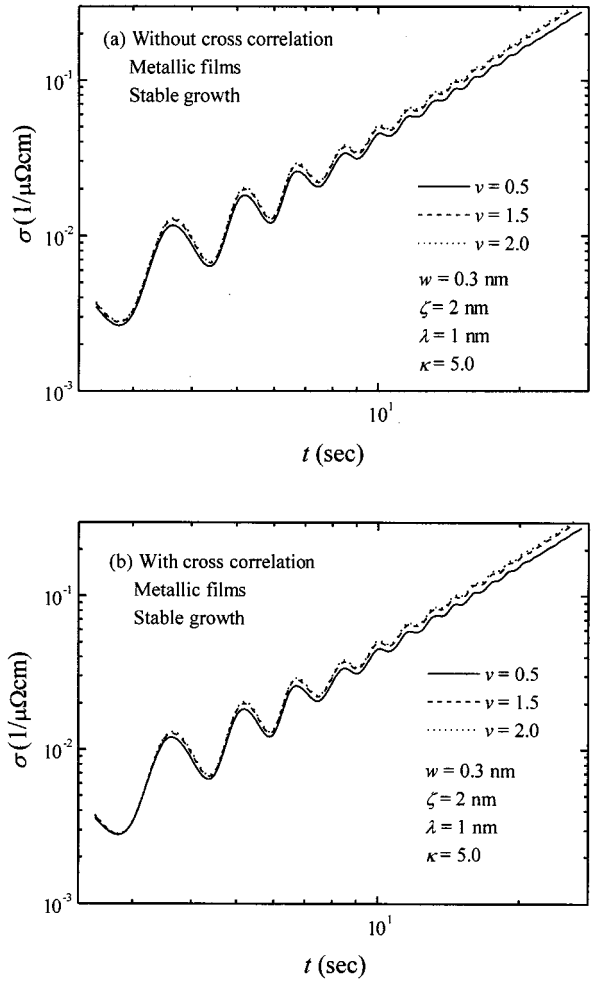

FIG. 6. Log-log plot of the conductivity σ of a thin metallic film vs growth time t (stable growth) for different v values: $v=0.5$, 1.5, and 2 (a) without cross correlation, and (b) with cross correlation contribution. Here, the roughness parameters of the substrate are $w=0.3$ nm, $\zeta=2$ nm, $\lambda=1$ nm; and $\kappa=5.0$, and the electron density $n=4.8\times10^{1}$ nm^{-3}.

The contribution of nonzero cross correlation [Fig. 5(b)] alters the conductivity behavior at early stages of growth where QSE oscillations are significant. If we go back to the cross correlation Eq. (6), for the unstable growth, the power spectrum of spatial frequency $q<q_0$ will be amplified while high spatial frequency part $q>q_0$ will be suppressed. For initial growth, contribution from the growth front roughness is small compared to the growing substrate roughness contribution. At this stage, substrate effect dominates the conductivity. However, as the growth time increases, the growth front roughness will take over, and long-time behaviors of the conductivity with or without cross correlation should be the same, which is the case in Fig. 5.

Stable Growth. In the stable growth regime for $\zeta>\lambda$, Fig. 6 shows that the conductivity increases with increasing evaporation/condensation coefficient v, while the shape of QSE oscillations is preserved. For the stable growth, the surface becomes smoother when v becomes larger, which implies weaker surface/interface scattering, and the conductivity increases with growth time. For stable growth the effect of cross correlation is less significant for the substrate parameters considered [Fig. 6(b)]. On the other hand, in the stable growth regime, the long time behavior of the conductivity obeys a power law as a function of growth time, $\sigma\sim t^{s'}$. Without cross correlation, at large t (>10 s), for $v=2.0$, $s'=1.98$, and for $v=0.5$, $s'=1.93$; with cross correlation, for $v=2.0$, $s'=1.97$, and for $v=0.5$, $s'=1.94$. This qualitatively agrees with our prediction mentioned in the introduction and shows that the dynamic power law behavior of the conductivity can be affected by different growth modes. However, the discussion in the introduction was very crude, because we did not consider the change of the lateral correlation length. For example, after $t>10$ s, the lateral correlation length ξ for $v=2.0$ should be larger than $\sqrt{2vt}\approx0.6$ nm. From the discussion in Sec. IV, one finds $\xi q_F>7.5$ after $t=10$ sec. If there is no change in both w and ξ, we would expect $s'\approx1.91$ from Sec. IV. From the discussion in the introduction, we would expect an s' less than 1.91. However Fig. 6(a) gives an s' value larger than 1.91. Therefore, the growth of the lateral correlation length has a great impact on the conductivity behavior. This effect becomes even more pronounced when the substrate is rough. This may provide a clue to solve the contradiction in the interpretation of the experimental conductivity of CoSi.[14]

Fishman and Calecki used a Gaussian correlation function to interpret the experimental result of CoSi.[14] Their best fit showed that $w=4$ Å and $\xi=2$ Å. Under this condition, since $\xi q_F\sim1$, $s\sim2.3$, which gives a remarkably good fit of the experimental data. However, the morphological parameters they obtained are quite unphysical. Because $\xi=2$ Å is smaller than the lattice constant of CoSi (~3 Å), the surface should be very smooth ($w\sim0$). But their $w=4$ Å contradicts this expectation. In addition, the average local slope $w/\xi=2$ (which means a surface has mounds with an average contact angle of 63.5°) is too large to be realistic. They also tried different correlation functions (both Gaussian and exponential) with different ξ. The exponent s decreases as ξ increases. For $\xi=10$ Å, $s=1.5$, which is far below the value obtained experimentally.[14] All these considerations are based on the assumption that at any thickness the CoSi films have the same w and ξ, and these could not explain the experimental results. Our results show that even under the condition of $\xi q_F\gg1$, if we include the dynamic growth effect during CoSi film growth, as well as the substrate roughness effect, we can still obtain an exponent s' very close to the experimental results. Figure 7 plots the experimental data presented in Ref. 14 and our model fit by assuming an exponentially-decaying auto-correlation function. We assume that both w and ξ are functions of film thickness d, and $w<\xi$ for any thickness. To our knowledge, there is no detailed study of dynamics roughening on solid-phase epitaxy. Since it is a deposition process followed by an annealing process, it is reasonable that the w will become smaller while ξ will increase for larger film thickness d. When $w=14.8d^{-0.22}$, and $\xi=16.44d^{0.23}$, the best fit gives $s'=2.4$, which is about the same as that obtained by Fishman and Calecki.[14] Therefore, dynamic roughening process plays a very important role in the thickness dependent conductivity.

In addition, the different s' values for different v imply that at different growth temperatures, one may expect a different power law for the thickness or growth time dependent

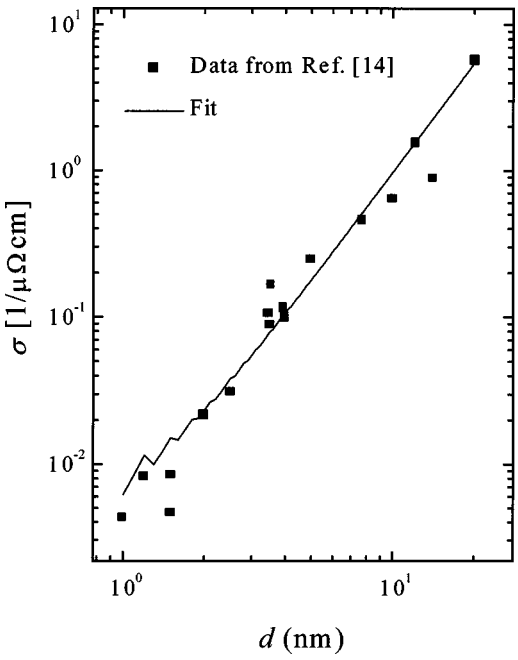

FIG. 7. Our fit (solid curve) to the experimental data (filled squares) presented in Ref. 14. We assume an exponentially-decaying auto-correlation function, and that both w and ξ are functions of film thickness d. The best fit gives $\sigma \propto d^{2.4}$, when $w = 14.8d^{-0.22}$, and $\xi = 16.44d^{0.23}$.

conductivity, given that the measuring temperature of the conductivity is the same. For example, at high temperatures, the growth is under thermal equilibrium, and one would expect a very smooth surface. In this case since $w \sim 0$, and $\xi \sim 0$, one would expect a very good theoretical explanation without considering the dynamic roughening process. However, if the growth is performed under low temperature, the dynamic roughening process cannot be ignored.

Comparing Fig. 5 with Fig. 6, we can see that the unstable growth may give anomalous behavior of thickness-dependent or growth time dependent conductivity, in addition to the initial percolation transition from discontinuous film to a percolated and continuous film. This is because the exponential increase of w overcomes the growth of the lateral correlation length ξ at long time, and the local slope increases dramatically with time.

VI. CONCLUSIONS

In conclusion, we studied in detail the influence of surface/interface roughness on the electrical conductivity of semiconducting and metallic films. We consider of thin films with a single rough mound boundary and with two rough boundaries. For semiconducting films with a single rough boundary and when only one miniband is occupied, the electron scattering is due to the intraminiband scattering. The intraminiband cutoff q_c limits the contribution from mound surface scattering. Three different cases are illustrated to show how surface morphology affects the conductivity: $q_0 < q_c$, $q_0 = q_c$, and $q_0 > q_c$. For $q_0 > q_c$, the center of the power spectrum is outside the scattering wave vector. At large $\zeta > \lambda$, there is no contribution from the mound surface to the conductivity. For $q_0 = q_c$, there is always half of the power spectrum contributing to the electron scattering. At very large $\zeta \gg \lambda$, since the mound separation is compatible to the wavelength of the scattered electron, the backward scattering probability of electrons reaches its maximum, and the conductivity becomes a minimum. For $q_0 < q_c$, the entire power spectrum contributes to the scattering. However, at large $\zeta > \lambda$, q_0 is the only scattering wave vector that electron can chose, and the conductivity saturates.

For a single boundary metallic film, QSE oscillations are shifted in phase and weakened by the presence of wavelength selection in surface morphology. Since the miniband-edge wave vector q_v is usually much larger than the q_0, those effects mainly come from the electron interminiband scattering. In this case, the conductivity shows a minimum as a function of ζ for $\lambda > \lambda_F$ and/or $\lambda < \lambda_F$ (with λ_F being the Fermi wavelength).

The formation of the double rough boundaries is considered through linear (stable and unstable) Langevin equations, which allow an estimation of cross-correlation electron scattering effects. The presence of cross correlation and the film growth mode were shown to influence significantly the film conductivity, as well as the size and shape of quantum size effects. For unstable growing surfaces, the conductivity is sensitive to the Schwoebel barrier coefficient v, which strongly modifies the shapes and sizes of QSE oscillations. In the stable growth regime, on the other hand, the shape of QSE oscillations in conductivity is preserved. We also have shown that even under the condition $\xi q_F \gg 1$, the power-law dependence of the conductivity versus film thickness (growth time) can still give a large exponent ($s' \approx 2.0$), which may provide a way to explain some experimental results.

Finally, we should mention that the behavior of the electrical conductivity as a function of thin-film growth time is a result of the competition between the thickness increment, and the roughness variation with growth time. If the roughness increment is slower than the thickness growth, then the QSE oscillation preserves during growth, like in the stable growth case. On the other hand, if the roughness increases much faster than the film thickness, the loss of the conductivity caused by boundary roughness scattering will overcome the gain by the increment of the thickness, and the QSE oscillations may diminish. In addition, we should emphasize that the growth models we considered in this paper are very simple, which may not be the case in reality, especially for unstable growth since here we considered only the early stage of the step barrier effect. Nevertheless, these two simple models demonstrate in principle how different growth modes will affect the conductivity behavior of growing thin films.

ACKNOWLEDGMENTS

G.P. would like to acknowledge support from the Netherlands Institute for Metals Research (NIMR), and Y. Tokura's critical reading of the manuscript and important comments. Work at Rensselaer was supported by the NSF and the Semiconductor Industrial Association Focus Center Research Program, J.B. acknowledges support through Research Project No. 2P03B 075 14 of the Polish State Research Committee.

[1] V. B. Sandomirskii, Zh. Eksp. Teor. Fiz. **52**, 158 (1967) [Sov. Phys. JETP **25**, 101 (1967)].
[2] C. R. Tellier and A. J. Tosser, *Size Effects in Thin Films* (Elsevier, New York, 1982) and references therein; J. J. Thompson, Proc. Cambridge Philos. Soc. **11**, 1120 (1901); K. Fuchs, *ibid.* **34**, 100 (1938); E. H. Sondheimer, Adv. Phys. **1**, 1 (1952).
[3] M. Jalochowski and E. Bauer, Phys. Rev. B **38**, 5272 (1988); M. Jalochowski, E. Bauer, H. Knoppe, and G. Lilienkamp, *ibid.* **45**, 13 607 (1992); M. Jalochowski, M. Hoffmann, and E. Bauer, Phys. Rev. Lett. **76**, 4227 (1996).
[4] M. Jalochowski and E. Bauer, Phys. Rev. B **37**, 8622 (1988).
[5] G. Fischer and H. Hoffmann, Z. Phys. B: Condens. Matter **39**, 287 (1980); H. Hoffmann and G. Fischer, Thin Solid Films **36**, 25 (1976).
[6] D. Schumacher and D. Stark, Surf. Sci. **123**, 384 (1982).
[7] E. Z. Luo, S. Heun, M. Kennedy, J. Wollschläger, and M. Henzler, Phys. Rev. B **49**, 4858 (1994).
[8] H. Sakaki, T. Noda, K. Hirakawa, M. Tanaka, and T. Matsusue, Appl. Phys. Lett. **51**, 1934 (1987).
[9] S. M. Goodnick, D. K. Ferry, C. W. Wilmsen, Z. Liliental, D. Fathy, and O. L. Krivanek, Phys. Rev. B **32**, 8171 (1985).
[10] G. H. Kruithof, T. M. Klapwijk, and S. Bakker, Phys. Rev. B **43**, 6642 (1991).
[11] R. M. Feenstra, D. A. Collins, D. Z.-Y. Ting, M. W. Wang, and T. C. McGill, Phys. Rev. Lett. **72**, 2749 (1994).
[12] K. M. Leung, Phys. Rev. B **30**, 647 (1984).
[13] N. Trivedi and N. W. Ashcroft, Phys. Rev. B **38**, 12 298 (1988).
[14] G. Fishman and D. Calecki, Phys. Rev. Lett. **62**, 1302 (1989); G. Fishman and D. Calecki, Phys. Rev. B **43**, 11 581 (1991).
[15] C. Kunze, Solid State Commun. **87**, 359 (1993).
[16] L. Sheng, D. X. Xing, and Z. D. Wang, Phys. Rev. B **51**, 7325 (1995).
[17] A. Kaser and E. Gerlach, Z. Phys. B: Condens. Matter **97**, 139 (1995); **98**, 207 (1995).
[18] G. Palasantzas and J. Barnas, Phys. Rev. B **56**, 7726 (1997); J. Barnas and G. Palasantzas, J. Appl. Phys. **82**, 3950 (1997); G. Palasantzas and J. Barnas, Phys. Status Solidi B **209**, 319 (1998).
[19] J. C. Hensel, R. T. Tung, J. M. Poate, and F. C. Unterwald, Phys. Rev. Lett. **54**, 1840 (1985); P. A. Badoz, A. Briggs, E. Rosencher, F. A. d'Avitaya, and C. d'Anterroches, Appl. Phys. Lett. **51**, 169 (1985); J. Y. Duboz, P. A. Badoz, E. Rosencher, J. Henz, M. Ospelt, H. von Känel, and A. A. Briggs, *ibid.* **53**, 788 (1988); R. G. P. van der Kraan, J. F. Jongste, H. M. Laeger, G. C. A. M. Janssen, and S. Radelaar, Phys. Rev. B **44**, 13 140 (1991).
[20] F. Rosenberger, in *Interfacial Aspects of Phase Transformations*, edited by B. Mutaftschiev (Reidel, Dordrecht, 1982).
[21] T. Halpin-Healy and Y.-C. Zhang, Phys. Rep. **254**, 215 (1995).
[22] J. Villain, J. Phys. I **1**, 19 (1991); M. D. Johnson, C. Orme, A. W. Hunt, D. Graff, J. Sudijono, L. M. Sander, and B. G. Orr, Phys. Rev. Lett. **72**, 116 (1994); M. Siegert and M. Plischke, *ibid.* **73**, 1517 (1994); J.-K. Zuo and J. F. Wendelken, Phys. Rev. Lett. **78**, 2791 (1997); J. A. Stroscio, D. T. Pierce, M. D. Stiles, A. Zangwill, and L. M. Sander, *ibid.* **75**, 4246 (1995); P. E. Hageman, H. J. W. Zandvliet, G. A. M. Kip, and A. van Silfhout, Surf. Sci. **311**, L655 (1994); J. E. van Nostrand, S. J. Grey, M.-A. Hasan, D. G. Cahill, and J. E. Greene, Phys. Rev. Lett. **74**, 3164 (1996).
[23] *Dynamics of Fractal Surfaces*, edited by F. Family and T. Vicsek (World Scientific, Singapore, 1990); P. Meakin, Phys. Rep. **235**, 1991 (1993); H.-N. Yang, G.-C. Wang, and T.-M. Lu, *Diffraction from Rough Surfaces and Dynamic Growth Fronts* (World Scientific, Singapore, 1993); J. Krim and G. Palasantzas, J. Mol. Struct. **9**, 599 (1995); A.-L. Barabasi and H. E. Stanley, *Fractal Concepts in Surface Growth* (Cambridge University Press, New York, 1995).
[24] Y.-P. Zhao, H.-N. Yang, G.-C. Wang, and T.-M. Lu, Phys. Rev. B **57**, 1922 (1998).
[25] J. Barnas and Y. Bruynseraede, Europhys. Lett. **32**, 167 (1995).
[26] J. Barnas and Y. Bruynseraede, Phys. Rev. B **53**, 5449 (1996).
[27] A. E. Meyerovich and A. Stepaniats, Phys. Rev. B **60**, 9129 (1999); G. Palasantzas and J. Barnas (unpublished).